HHS Public Access

Author manuscript

Nature. Author manuscript; available in PMC 2012 October 12.

Published in final edited form as:

Nature. ; 484(7393): 265–269. doi:10.1038/nature10916.

Visualising molecular juggling within a B_{12}-dependent methyltransferase complex

Yan Kung[1], **Nozomi Ando**[1], **Tzanko I. Doukov**[1,4], **Leah C. Blasiak**[1,5], **Güneş Bender**[6], **Javier Seravalli**[7], **Stephen W. Ragsdale**[6], and **Catherine L. Drennan**[1,2,3,*]

[1]Department of Chemistry, Massachusetts Institute of Technology, Cambridge, MA 02139

[2]Department of Biology, Massachusetts Institute of Technology, Cambridge, MA 02139

[3]Howard Hughes Medical Institute, Massachusetts Institute of Technology, Cambridge, MA 02139

[6]Department of Biological Chemistry, University of Michigan, Ann Arbor, MI 48109

[7]Department of Biochemistry, University of Nebraska, Lincoln, NE 68588

Abstract

Derivatives of vitamin B_{12} are used in methyl group transfer in biological processes as diverse as methionine synthesis in humans and CO_2 fixation in acetogenic bacteria[1–3]. This seemingly straightforward reaction requires large, multimodular enzyme complexes that adopt multiple conformations to alternately activate, protect, and perform catalysis on the reactive B_{12} cofactor. Crystal structures determined thus far have provided structural information for only fragments of these complexes[4–12], inspiring speculation regarding the overall protein assembly and conformational movements inherent to activity. Here we present X-ray crystal structures of a complete ~220 kDa complex that contains all enzymes responsible for B_{12}-dependent methyltransfer, namely the corrinoid iron-sulfur protein (CFeSP) and its methyltransferase (MeTr) from the model acetogen *Moorella thermoacetica*. These structures provide the first three-dimensional depiction of all protein modules required for the activation, protection, and catalytic steps of B_{12}-dependent methyltransfer. In addition, the structures capture B_{12} at multiple locations between its "resting" and catalytic positions, allowing visualisation of the dramatic protein rearrangements that enable methyltransfer and identification of the trajectory for B_{12} movement within the large enzyme scaffold. The structures are also presented alongside *in crystallo* UV-vis

*Corresponding author cdrennan@mit.edu, Tel: 617-253-5622, Fax: 617-258-7847.

[4]Present address: Stanford Synchrotron Radiation Lightsource, Menlo Park, CA 94025

[5]Present address: Institute of Marine and Environmental Technology, University of Maryland, Center for Environmental Science, Baltimore, MD 21202

Supplementary Information is linked to the online version of the paper at www.nature.com/nature.

Author Contributions Y.K. performed crystallization and data collection, processing, and refinement that gave the folate-free and folate-bound CFeSP/MeTr structures. N.A. built the microspectrophotometer and performed *in crystallo* UV-vis experiments with the aid of Y.K., who performed the parallel solution UV-vis experiments. T.I.D. determined initial crystallization conditions and performed initial data collection, and L.C.B. processed and refined these data. G.B. and J.S. expressed and purified protein samples, and S.W.R and C.L.D. were involved in study design. Y.K. and C.L.D. wrote the manuscript.

Author Information Atomic coordinates are deposited in the Protein Data Bank under accession codes XXXX, XXXX, and XXXX. Reprints and permissions information is available at www.nature.com/reprints. The authors declare no competing financial interests.

spectroscopic data, which confirm enzymatic activity within crystals and demonstrate the largest known conformational movements of proteins in a crystalline state. Taken together, this work provides a model for the molecular juggling that accompanies turnover and helps explain why such an elaborate protein framework is required for such a simple, yet biologically essential reaction.

B_{12}-dependent methyltransfer lies at the heart of methylation biochemistry and is an essential reaction in human health and microbial CO_2 sequestration[2,3]. In humans, methionine synthase (MetH) methylates homocysteine to form methionine to maintain cellular pools of folate (vitamin B_9) and *S*-adenosylmethionine (AdoMet), the universal methyl donor. MetH mutation or vitamin B_{12} deficiency can cause serious health consequences, including megaloblastic anemia and birth abnormalities such as neural tube defects[13]. Acetogenic bacteria, including *M. thermoacetica*, use CFeSP and MeTr together to catalyze methyltransfer in the Wood-Ljungdahl carbon fixation pathway for growth on CO_2 as the sole carbon source[14].

For both MetH and CFeSP/MeTr, methyltetrahydrofolate (CH_3-H_4folate) is the methyl donor, and a protein-bound B_{12} derivative (cobalamin for MetH and 5′-methoxybenzimidazolyl cobamide for CFeSP) is the methyl carrier. In acetogenic bacteria, the CH_3-H_4folate methyl group is derived from enzymatic reduction of CO_2, whereas in humans, CH_3-H_4folate is the predominant circulating form of the vitamin. Although CH_3-H_4folate is the common methyl source, methyl removal from the N^5 tertiary amine is chemically challenging because the product, tetrahydrofolate (H_4folate), is a poor leaving group[1]. Therefore, a particularly powerful nucleophile is required, and B_{12} with cobalt in the +1 oxidation state, a Co(I) species dubbed a “supernucleophile”[15], is recruited. Such strong reactivity comes at a price: reducing the inactive Co(II) state to active Co(I) is thermodynamically challenging, as the Co(II/I) reduction potential is one of the lowest in nature, −504 mV in CFeSP and −526 mV in MetH[16,17]. In CFeSP, an electron is first delivered from a partner protein to an Fe_4S_4 cluster harboured by an activation domain[18,19]. The electron is then passed to Co(II) to yield Co(I) (Eq. 1), which attacks CH_3-H_4folate to form CH_3-Co(III) (Eq. 2). CFeSP then delivers the methyl group to the $Ni_2Fe_4S_4$ active site metallocluster (A-cluster) of acetyl-CoA synthase (ACS), where it becomes the methyl of acetyl CoA, and B_{12} returns to its nucleophilic Co(I) state.

$$[4\mathrm{Fe}-4\mathrm{S}]^{1+}+\mathrm{Co(II)} \rightleftarrows [4\mathrm{Fe}-4\mathrm{S}]^{2+}+\mathrm{Co(I)} \quad \text{(Eq. 1)}$$

$$\mathrm{Co(I)}+\mathrm{CH_3}-\mathrm{H_4folate} \rightleftarrows \mathrm{CH_3}-\mathrm{Co(III)}+\mathrm{H_4folate} \quad \text{(Eq. 2)}$$

During the catalytic cycle of both MetH and CFeSP/MeTr (Supplementary Fig. 1), a series of “molecular juggling” acts must be carried out in which domains rearrange to contact the B_{12} cofactor. Crystal structures of a MetH B_{12}-binding fragment[4] and CFeSP from *Carboxydothermus hydrogenoformans* (*Ch*CFeSP)[9] both depict a “resting” state, where B_{12} is buried by a protective “capping” domain, shielded from unwanted chemistry but inaccessible to substrate. Because methyltransfer employs S_N2 substitution[20], large

conformational changes must "uncap" B_{12} before chemistry can occur. B_{12} is "uncapped" in structures of MetH fragments that depict B_{12} activation[7,11,12], but no structure has been solved that shows B_{12}- and CH_3-H_4folate-binding domains together to illustrate methyltransfer.

To visualise this elusive methyltransfer complex, we determined a 2.38 Å resolution structure of folate-free CFeSP/MeTr from *M. thermoacetica* (Fig. 1, Supplementary Table 1). The homodimeric MeTr component (58 kDa) is virtually identical to prior structures of both MeTr[6,10] (Supplementary Fig. 2a), rms deviation for Cα atoms (rmsd): 0.39 Å, and the analogous MetH domain that binds CH_3-H_4folate[8], rmsd: 1.03–1.08 Å. MeTr and MetH both use $(\beta/\alpha)_8$ triosephosphate isomerase (TIM) barrels to bind and activate CH_3-H_4folate for nucleophilic attack. Two CFeSPs are present in the complex, each containing two subunits. The small subunit (35 kDa) is a TIM barrel which acts as the B_{12} "cap" in the *Ch*CFeSP structure[9], while the large subunit (48 kDa) has three domains joined by linkers: an N-terminal Fe_4S_4 activation domain (residues 1–57), a TIM barrel domain (residues 93–312), and a C-terminal B_{12}-binding domain (residues 325–446). With the exception of Fe_4S_4- and B_{12}- domains, discussed below, both CFeSP copies align well to the *Ch*CFeSP structure, rmsd: 0.81–0.85 Å (Supplementary Fig. 2b).

In the ~220 kDa CFeSP/MeTr assembly (Fig. 1), the MeTr homodimer lies in the centre, with one CFeSP bound on either side. Each MeTr monomer has a C-terminal α-helix (residues 255–262) protruding from the TIM barrel rim. Contacts between this helix and its preceding loop with a CFeSP small subunit helix (residues 191–204) form the primary interactions between MeTr and CFeSP (Supplementary Fig. 3). Weak interactions between MeTr and CFeSP Fe_4S_4-domains have stabilized these highly flexible[9] domains responsible for B_{12} activation, allowing their visualisation as bundles of short α-helices connected by long loops that coordinate the Fe_4S_4 cubane (Fig. 1 and Supplementary Figs. 4–5). The Fe_4S_4-domains are observed to adopt a variety of positions that are all too far from the B_{12} to afford reductive activation[9]. However, the long and primarily unstructured protein linkers that connect both the Fe_4S_4- and B_{12}- domains to the central TIM barrel must allow for the requisite flexibility for B_{12} activation (Supplementary Figs. 2b, 6).

B_{12}-domains of both MetH and CFeSP adopt Rossmann-like architectures that bind B_{12} in the base-off conformation (Fig. 1)[4,9]. High *B*-factors support the notion of flexibility mentioned above (Supplementary Fig. 7, Supplementary Table 2), where electron density for both B_{12}-domains represents a highest occupancy position within an ensemble, rather than a sole conformation. In both CFeSPs, the average B_{12}-domain position resides between the "capping" small subunit TIM barrel and the TIM barrel of a MeTr monomer, which are adjacent and nearly perpendicular to each other (Fig. 1). On average, the B_{12} Co has shifted ~6.5 Å away from its "resting" location towards the MeTr folate-binding site. B_{12} in this structure is thus positioned "en route" towards catalysis, with ~18 Å remaining to the methyl group of folate modeled into the MeTr active site, based on an alignment with the folate-bound MeTr structure[10]. In transitioning between "resting" and "en route" positions, the B_{12} corrin ring breaks three interactions with the "capping" domain and forms new contacts, including an H bond with Asn203 of MeTr (Fig. 2a-b).

Given the flexibility suggested by this structural analysis, we explored whether the B_{12} domain can sample the full ~25 Å to afford turnover within intact crystals, using anaerobic *in crystallo* UV-vis spectroscopy to monitor the state of B_{12}. *In crystallo* and analogous solution spectra were collected in parallel (Fig. 3) for the as-isolated Co(II) form of B_{12}. Reduction to Co(I) and methylation to CH_3-Co(III) were then achieved *in crystallo* and in solution, with all spectra matching well-established CFeSP UV-vis features[18,19,21–23]. Importantly, absorption features disappear when light is passed through the solution surrounding the crystals, indicating that spectra represent protein in crystals and not protein that may have been liberated into the solution. Collectively, these data demonstrate enzymatic transfer of the CH_3-H_4folate methyl group to CFeSP-bound B_{12}, evidence that the B_{12}-domain is able to move at least ~18 Å to trigger methyltransfer within the crystal. To our knowledge, this conformational movement represents the largest observed in a crystallized protein (Supplementary Discussion). Such dramatic B_{12}-domain movement is likely facilitated by the fact that the majority of CFeSP/MeTr is composed of rigid TIM barrels that provide all the lattice contacts (Supplementary Fig. 8). Although their biosynthesis is energetically expensive, these high molecular weight TIM barrel scaffolds may be important for B_{12}-dependent methyltransferases to maintain structural integrity during the conformational gymnastics that alternately enable activation, protection, and catalysis of the highly reactive B_{12} cofactor. Thus, despite the small size of the transferred methyl moiety, these large conformational changes appear to necessitate large enzyme sizes.

While the folate-free CFeSP/MeTr structure describes large B_{12}-domain movements that "uncap" B_{12} from the small subunit, it is interesting to consider why binding of CFeSP to MeTr does not simply position the B_{12}-domain directly over the MeTr active site. One explanation is that the structure represents an inactive complex; however, *in crystallo* results clearly demonstrate that CFeSP/MeTr crystals are active. Another explanation posits that an ensemble of "en route" conformations exists when CH_3-H_4folate is absent, and that CH_3-H_4folate binding would shift the conformational equilibrium, moving B_{12} closer to the folate-binding site. To obtain experimental support for this hypothesis, we solved additional CFeSP/MeTr structures co crystallized with CH_3-H_4folate, with and without Ti(III) citrate as a reductant at 3.03 Å and 3.50 Å resolution, respectively. UV-vis spectroscopy performed on these crystals shows that these structures represent a substrate form (CH_3–H_4folate bound, B_{12} in the Co(II) state) and a product form (H_4folate bound, B_{12} in the CH_3 Co(III) state) of the complex (Supplementary Fig. 9). Compared with the folate-free structure, B_{12} in both folate-bound structures has indeed moved even closer to the MeTr folate-binding site (by an average of ~7.7 Å) and exhibits new H bonding features (Fig. 2c). In these folate-bound structures, the B_{12} corrin ring has severed all interactions with the "capping" CFeSP small subunit and contacts only MeTr residues. Here, asparagine and glutamine residues that line the MeTr surface appear to participate in an "amide hand off", sequentially passing B_{12} along its trajectory as it progresses towards folate (Fig. 2b-c and Supplementary Fig. 10).

Interestingly, the terminal amide in this "hand off", Asn199, is strictly conserved in both MeTr and MetH and was previously shown to switch conformations between folate-free and folate-bound forms[10], a feature also observed in the CFeSP/MeTr structures presented here (Fig. 2b-c,e). In apo-MeTr structures, Asn199 points upwards and out of the active site,

while in folate-bound MeTr structures Asn199 turns down to H-bond with the N^5 of folate. Since N199A mutation moderately affects folate binding (20-fold in K_d) but dramatically compromises catalytic efficiency (25,000-fold in k_{cat}/K_m), Asn199 is thought to be important for formation of the transition state[10]. In our CFeSP/MeTr structures, we observe a new role for Asn199 in B_{12}-domain conformational switching: when folate is absent, Asn199 points out of the active site, blocking a closer B_{12} position. However, when folate binds and Asn199 reorients to H-bond with folate, space becomes available for B_{12} to move closer to the MeTr folate-binding site. Therefore, the position of Asn199 itself could help shift the conformational equilibrium of the B_{12}-domain, signalling that substrate has bound to MeTr. Asn199 is an ideal signal for substrate binding, as it is the only MeTr residue known to reposition upon folate binding[10].

Displacement of the B_{12}-domain from its resting position to the position nearest the folate-binding site can be attributed to two independent conformational changes within the complex, best described as “swinging” and “clamping” motions (Fig. 2d). The B_{12}-domain can “swing” relative to the rest of CFeSP (Supplementary Fig. 11), and CFeSP can “clamp” the B_{12}-domain towards the MeTr active site (Fig. 2d, Supplementary Fig. 12). Despite varying degrees of “clamping” over a range of ~14° across the structures, the interface between the CFeSP small subunit and MeTr is preserved (Supplementary Fig. 13).

Although folate binding shifts the average position of the B_{12}-domain closer to the MeTr folate-binding site, the B_{12} Co is still too far for S_N2 methyl transfer (Figure 2e). Intriguingly, a large, continuous electron density peak is present in $2F_o$-F_c, F_o-F_c, and composite omit maps, emanating from the corrin ring and stretching directly over the folate-binding site, suggestive of an alternative, low-occupancy corrin conformation (Fig. 2f, Supplementary Fig. 14). A trial refinement of a putative corrin ring at 40% occupancy satisfies the F_o-F_c difference maps (Supplementary Fig. 15), positioning B_{12} over the folate-binding site.

The multiple positions of B_{12} captured here (Fig. 2g) highlight the conformational flexibility of the CFeSP/MeTr scaffold and provide a framework to understand the molecular juggling of domains during B_{12}-dependent methyltransfer (Fig. 4). Prior to MeTr binding, the CFeSP B_{12}-domain rests against the “capping” small subunit, as in the structure of *Ch*CFeSP[9], with reactive Co(I) of B_{12} protected (“resting” state). From this conformation, either the “cap” or the B_{12}-domain must move to allow substrate access. Our folate-free CFeSP/MeTr structure indicates that upon MeTr binding, the B_{12}-domain becomes “loosened” and flexible, adopting an ensemble of conformations that lie en route towards the MeTr active site. Here, reactive B_{12} species would be protected by the CFeSP small subunit and MeTr TIM barrels. CH_3-H_4folate binding to MeTr accompanied by movement of Asn199 shifts the equilibrium of B_{12}-domain conformers, placing B_{12} closer to folate, as in our folate-bound CFeSP/MeTr structures, with B_{12} protection afforded by MeTr. It is notable that even after CH_3-H_4folate binds, the major B_{12} position is still not directly over the folate methyl group, as such a position is expected to be transient. After methyltransfer, the B_{12}-domain can return to the small subunit to “re-cap” the methylated B_{12} product, protected by the small subunit TIM barrel.

Overall, our data indicate that B_{12}-domain movement is not a simple, two-state switch between "resting" and "catalytic" conformations. Instead, a flexible B_{12}-domain samples an ensemble of conformations, where subtle shifts of the conformational equilibrium place B_{12} progressively closer to the active site, thereby increasing the population of conformers capable of methyltransfer without obstructing substrate access or hindering domain movement. This model is consistent with MetH studies where ligation, alkylation, and redox state of the B_{12} cobalt can favour/disfavour various binding modes, alternately shifting the equilibrium of conformers for ordered domain rearrangements during the reaction cycle[11,12,24,25]. We further identify MeTr residues that contact B_{12} along its trajectory, ending with Asn199. In MetH the B_{12} ligating residue His759 has been shown to play a dual role in catalysis and in signalling conformational shifts[11]. The strictly conserved, folate binding Asn199 of MeTr could similarly play a dual role in both catalysis and conformational signalling. We thus expect this model for dynamic domain juggling, communicated by residues involved in substrate and cofactor binding, to be a common theme in methyltransfer between the B vitamins folate and B_{12}.

Methods Summary

CFeSP and MeTr were expressed and purified anaerobically from *M. thermoacetica* ATCC 39073 and from recombinant *Escherichia coli*, respectively. Crystals were grown anaerobically by hanging drop vapour diffusion. Diffraction data were collected at 24ID-C at the Advanced Photon Source, Argonne National Laboratory, and 5.0.2 and 8.2.2 at the Advanced Light Source, Lawrence Berkeley National Laboratory. Structures were solved by molecular replacement. Data collection and refinement statistics are presented in Supplementary Table 1, and representative electron density for protein domains and for cofactors/substrate are shown in Supplementary Figs. 16–21. Solution and *in crystallo* UV-vis absorption spectra were collected as described in the text and in the Full Methods.

Full Methods and any associated references are available in the online version of the paper at www.nature.com/nature.

Methods

Protein Purification

CFeSP was expressed and purified anaerobically from *Moorella thermoacetica* ATCC 39073 as described[21], except for the following modifications. CFeSP was purified from cell extracts using DEAE-cellulose and high resolution Q-Sepharose anion exchange chromatography followed by phenyl-Sepharose hydrophobic interaction chromatography. Fractions containing CFeSP were concentrated and buffer exchanged using Amicon ultracentrifuge concentrators in the anaerobic chamber. MeTr was expressed and purified anaerobically from recombinant *Escherichia coli* as described[6]. Concentrations of CFeSP and MeTr protein samples were determined using the Rose-Bengal method[28] and kept in storage buffer: 50 mM Tris-HCl, pH 7.6, 100 mM NaCl, 2 mM dithiothreitol.

Crystallization

Crystals of the folate-free CFeSP/MeTr complex were grown by hanging drop vapour diffusion in an anaerobic chamber (Coy Laboratories) at room temperature by adding 1 μL of precipitant (100 mM Bis-Tris, pH 6.5, 100 mM calcium acetate, 9% PEG 5000 monomethyl ether, 20% glycerol) to 2 μL of an equimolar mixture of CFeSP and MeTr (~250 μM monomer for each), over a 0.5 mL reservoir solution of precipitant. Large, brown, rod-shaped crystals appeared overnight. Crystals were looped and cryo-cooled in liquid nitrogen anaerobically prior to collection of X-ray diffraction data at 100 K. Crystals of CFeSP/MeTr co crystallized with the CH_3-H_4folate substrate were obtained in the same manner as above, except the protein solution also contained CH_3-H_4folate at 1 mM concentration. Crystals of CFeSP/MeTr co-crystallized with both CH_3-H_4folate and Ti(III) citrate as a reductant were obtained in the same manner, except the precipitant solution also contained Ti(III) citrate at 3 mM concentration.

Structure Determination of Folate-Free CFeSP/MeTr Structure

Two X-ray diffraction data sets were collected for the folate-free CFeSP/MeTr structure. A lower-resolution data set (3.3 Å) was collected at the Advanced Light Source (ALS) beam line 5.0.2 (λ=1.1000 Å), and a higher-resolution data set (2.38 Å) was later collected at the Advanced Photon Source (APS) beam line 24ID-C (λ=0.9792 Å).

The initial data set to 3.3 Å resolution was processed in HKL2000 and Scalepack[29]. The structure was solved by molecular replacement in Phaser[30], using individual structures of MeTr[10] (PDB ID: 2E7F) and *Ch*CFeSP[9] (PDB ID: 2H9A) lacking its B_{12}-domain as independent search models. Two CFeSP/MeTr complexes (~220 kDa each) were found in the asymmetric unit, and crystals belonged to the space group $P2_12_12_1$ with unit cell dimensions (Å): a=137.42, b=159.87, and c=241.92. Iterative rounds of refinement with residue-grouped *B*-factors were carried out in CNS[31] and PHENIX[32], with model building in Coot[33]. The four B_{12}-domains present in the complex were kept as a polyalanine model. Final R_{work} and R_{free} values for the model were 29.2% and 33.7%, respectively, when refinement of the structure to higher resolution began. Data collection and refinement statistics for this data set are shown in Supplementary Table 1. Ramachandran analysis was carried out in PROCHECK[34]: 74.0% of residues resided in the most favoured region, with 21.2% additionally allowed, 3.1% generously allowed, and 1.7% disfavoured.

The data set to 2.38 Å resolution was processed in HKL2000 and Scalepack[29]. Although this crystal formed in similar conditions as the crystal which gave the 3.3 Å resolution data set, the space group was now $P2_12_12$, with unit cell dimensions (Å): a=125.71, b=242.84, and c=79.67. The structure for this crystal was thus solved by molecular replacement in Phaser[30] using the MeTr homodimer and CFeSP heterodimers lacking B_{12}-domains from the previously refined model of the 3.3 Å resolution structure as independent search models. Only one CFeSP/MeTr complex was present in the asymmetric unit. Iterative rounds of refinement were carried out in CNS[31] and PHENIX[32], with model building in Coot[33]. Translation/libration/screw (TLS) refinement was carried out in latter refinement rounds with seven TLS groups: the MeTr homodimer (chains A and B), the Fe_4S_4 domain of one CFeSP large subunit (chain C), the TIM domain of chain C with one small subunit (chain

D), the B_{12} domain of chain C, the Fe_4S_4 domain of the second large subunit (chain E), the TIM domain of chain E with the second small subunit (chain F), and the B_{12} domain of chain E. Data collection and refinement statistics are shown in Supplementary Table 1, and average *B*-factors for each domain of the final model are given in Supplementary Table 2. Ramachandran analysis was carried out in PROCHECK[34]: 90.1% residues reside in the most favoured region, with 9.5% additionally allowed, 0.3% generously allowed, and 0.2% disfavoured. The final model contains residues 1–262 (of 262) for both MeTr chains (A and B), residues 2–442 (of 446) for both CFeSP large subunit chains (C and E), and residues 1–323 (of 323) for both CFeSP small subunit chains (D and F).

Except for the Fe_4S_4 and B_{12}-domains, the entire structure is composed of TIM barrels for which the electron density is well-defined (Supplementary Fig. 16). Electron density is weaker for the Fe_4S_4 domains (Supplementary Figs. 5, 17, and 19), consistent with the fact that these domains exhibit higher *B*-factors (Supplementary Table 2, Supplementary Fig. 7). However, reasonable electron density is present for the main chain and most side chains, allowing us to build a model for this domain. Still, several side chains of the Fe_4S_4 domains lack clear electron density, and thus for these residues, atoms were truncated past the Cβ atom (chain C: 12 residues truncated and chain E: 16 residues truncated, out of 56 total residues).

Although *B*-factors are high and electron density is weak for the B_{12}-domains in general, electron density for the B_{12} cofactors is unambiguous (Supplementary Fig. 20), and density is also clear in several helical regions, including those near B_{12} (Supplementary Fig. 18). Because the structure of a CFeSP B_{12}-domain bound with B_{12} was already known[9], we used the clear electron density of the B_{12} cofactor and the resolvable helices to position the B_{12}-domain during model building. Still, many side chains of the CFeSP B_{12}-domains lacked clear electron density, and thus for these residues, atoms were truncated past the Cβ atom (chain C: 50 residues truncated and chain E: 59 residues truncated, out of 118 total residues).

The B_{12} cofactor in the final model contains 5,6-dimethylbenzimidazole as the lower ligand moiety, as in cobalamin. Although active with cobalamin[35], previous studies have shown that CFeSP isolated from *M. thermoacetica* harbours an unusual B_{12} derivative that contains 5′ methoxybenzimidazole as the lower ligand instead[36]. However, disorder of the B_{12} cofactor and B_{12}-domain due to thermal motion of these regions in the CFeSP/MeTr crystal resulted in weak electron density for substituents of the benzimidazolyl ring (Supplementary Figs. 18 and 20). Therefore, we cannot confirm the presence of this unusual B_{12} derivative from our crystallographic studies, and we have thus modeled cobalamin as the form of B_{12} in the structure.

Previous spectroscopic studies[27] in addition to the crystal structure of *Ch*CFeSP[9] have indicated that a water molecule coordinates the central cobalt of B_{12} in the as-isolated CFeSP. Here, Co(II) is the major species and is expected to be five-coordinate. However, because of disorder we do not observe electron density to suggest a water molecule bound to cobalt (Supplementary Figs. 18 and 20). Accordingly, we have not modeled a water molecule.

Structure Determination of Folate-Bound CFeSP/MeTr Structures

For crystals grown with CH_3-H_4folate, X-ray diffraction data were collected at APS beam line 24ID-C to 3.50 Å resolution at λ=1.6039 Å to optimize the cobalt peak anomalous signal. For crystals grown with both CH_3-H_4folate and Ti(III) citrate, X-ray diffraction data were collected at ALS beam line 8.2.2 to 3.03 Å resolution at λ=1.0000 Å. The structures were solved by molecular replacement using the MeTr homodimer and CFeSP heterodimers lacking Fe_4S_4- and B_{12}-domains from the folate-free 2.38 Å CFeSP/MeTr structure as independent search models. Refinement of the folate-free CFeSP/MeTr structure against either folate bound X-ray data set was not sufficient to solve the structure, as the unit cell dimensions were markedly different (Supplementary Table 1). Following molecular replacement, one CFeSP/MeTr complex was present in the asymmetric unit, and omit electron density clearly indicated the presence of bound folate (Supplementary Fig. 21). Iterative rounds of refinement were carried out in CNS[31] and PHENIX[32], with model building in Coot[33]. The same test set of reflections for R_{free} calculations was used for both folate-bound data sets. Data collection and refinement statistics are shown in Supplementary Table 1. Ramachandran analysis was carried out in PROCHECK[34]: for the CH_3-H_4folate-only structure, 89.6% of residues reside in the most favoured region, with 9.8% additionally allowed, 0.3% generously allowed, and 0.2% disfavoured. For the CH_3-H_4folate with Ti(III) citrate structure, 89.5% of residues reside in the most favoured region, with 10.0% additionally allowed, 0.2% generously allowed, and 0.3% disfavoured. The final models both contain folate, B_{12} and residues 1–262 (of 262) for MeTr chains (A and B), residues 2–442 (of 446) for CFeSP large subunit chains (C and E), and residues 1–323 (of 323) for CFeSP small subunit chains (D and F). As with the folate-free structure, several side chains of the Fe_4S_4 domains for both folate-bound structures lacked clear electron density, and thus for these residues, atoms were truncated past the Cβ atom (chain C: 15 residues truncated and chain E: 18 residues truncated, out of 52 total residues). Similarly, many side chains of the B_{12}-domains lacked electron density, and thus for these residues, atoms were truncated past the Cβ atom (chain C: 51 residues truncated and chain E: 78 residues truncated, out of 118 total residues). The liganded/oxidation states of folate and B_{12} in these structures were determined by use of a UV-vis microspectrophotometer (see below).

Solution and *in crystallo* UV-visible Absorption Spectroscopy to Determine Enzyme Activity *in crystallo*

Titanium(III) citrate (100 mM in 50 mM Tris, pH 7.6) was prepared[37], and *(6S)-5*-methyl-*5,6,7,8*-tetrahydrofolate (CH_3-H_4folate) containing one glutamate tail was purchased from Schircks Laboratories. As-isolated, reduced, and methylated CFeSP samples in solution were prepared in a room temperature anaerobic chamber (MBraun) following similar procedures to those previously described[18,19,22,23,26,27]. Briefly, purified CFeSP (20 μM) was used for the as-isolated sample, CFeSP mixed with Ti(III) citrate (1 mM) was used for the reduced sample, and CFeSP mixed with equimolar MeTr, Ti(III) citrate (1 mM), and CH_3-H_4folate (1 mM) was used for the methylated sample. Spectra were taken using a Nanodrop 2000c (Thermo Scientific) in a quartz cuvette or on the sample stage in the anaerobic chamber directly after mixing; identical solutions lacking CFeSP were used as blanks.

To obtain *in crystallo* UV-vis spectra, CFeSP/MeTr crystals in as-isolated, reduced, and methylated forms were prepared in a similar fashion. In a room temperature anaerobic chamber (Coy Laboratories), crystals were looped into a 2 μL drop, which was placed on a cover slide and contained one of the following three solutions for as-isolated, reduced, and methylated samples, respectively: well solution, well solution with Ti(III) citrate (10 mM), and well solution with Ti(III) citrate (10 mM) and CH_3-H_4folate (1 mM). A ring of epoxy surrounding each drop was applied to the cover side, and a second cover slide was placed on top, sandwiching the drops within a uniform distance separation and sealing the crystals within an anaerobic environment. Upon curing of the epoxy, crystals were brought out of the anaerobic chamber and mounted on a an XZ translation stage (Newport, UMR8.25 & SM-13) in a fibre optic coupled microspectrophotometer (Ocean Optics, Jaz) with 40 mm diameter reflective objectives (Optique Peter, France) and a deuterium-halogen lamp (DH2000-BAL, Ocean Optics), similar to that previously described[38,39]. Stray light was blocked with black-out material. The light focus was coarsely aligned to the crystals by visual inspection and then finely aligned by monitoring light transmission in real time. Data were acquired at room temperature with the SpectraSuite software (Ocean Optics). The background transmission was measured through the solution immediately surrounding the crystals. The dark current was measured with the light shuttered off. Sample, reference, and dark current spectra were acquired by averaging 10–50 scans with total exposure times of 90–1000 ms. Experiments were completed within 60 min of sample preparation, and crystals remained intact over the course of the experiment, as observed using a microscope following data collection.

To generate Fig. 3, absorbance spectra were scaled relative to each other to account for variable crystal sizes and pathlengths, where absolute peak absorbances did not exceed 1 absorbance unit.

In crystallo UV-visible Absorption Spectroscopy on Folate-bound CFeSP/MeTr Crystals to Determine Liganded/Oxidation State of Bound B_{12} and Folate

UV-vis absorption spectra were collected on a microspectrophotometer at 100 K for crystals of folate-free CFeSP/MeTr, crystals that were grown in the presence of CH_3-H_4folate only, and for crystals grown in the presence of both CH_3 H_4folate and Ti(III) citrate (Supplementary Fig. 9). The spectra were compared to the analogous solution spectra (Fig. 3). The spectrum for the folate-free crystal is similar the spectrum of CFeSP alone in solution, with broad features at ~400 nm and 470 nm indicative of the Fe_4S_4 cluster and B_{12} primarily in the Co(II) state. The spectrum for the crystal grown with CH_3 H_4folate matches the spectrum of folate-free crystals, indicating that B_{12} has remained primarily in the Co(II) state, and turnover has not occurred. However, the spectrum for the crystal grown with both CH_3-H_4folate and Ti(III) citrate is markedly different and contains a peak at 450 nm, indicating that B_{12} in these crystals is methylated to the CH_3-Co(III) state. Based on these data, we have modeled the methyl group on folate in the structure co-crystallized with CH_3-H_4folate only, while we have modeled the methyl group bound to Co of B_{12} for the CH_3-H_4folate/Ti(III) citrate structure. Without these spectroscopic data, assignment of the location of the methyl group would have otherwise been prevented by the resolution limits of the data.

Supplementary Material

Refer to Web version on PubMed Central for supplementary material.

Acknowledgements

We thank Joseph E. Darty for his assistance to the purification of CFeSP. This work was supported by NIH grants GM69857 (C.L.D.) and GM39451 (S.W.R.) and the MIT Energy Initiative (C.L.D.). C.L.D. is a Howard Hughes Medical Institute Investigator. This work is based upon research conducted at the Advanced Photon Source on the Northeastern Collaborative Access Team beamlines, which are supported by award RR-15301 from the National Center for Research Resources at the National Institutes of Health. Use of the Advanced Photon Source is supported by the U.S. Department of Energy, Office of Basic Energy Sciences, under Contract No. DE-AC02-06CH11357. The Advanced Light Source is supported by the Director, Office of Science, Office of Basic Energy Sciences, of the U.S. Department of Energy under Contract No. DE-AC02-05CH11231.

References

1. Matthews RG. Cobalamin-Dependent Methyltransferases. Acc. Chem. Res. 2001; 34:681–689. [PubMed: 11513576]
2. Banerjee RB, Ragsdale SW. The Many Faces of Vitamin B12: Catalysis by Cobalamin-Dependent Enzymes. Annu. Rev. Biochem. 2003; 72:209–247. [PubMed: 14527323]
3. Matthews RG, Koutmos M, Datta S. Cobalamin-Dependent and Cobamide-Dependent Methyltransferases. Curr. Opin. Struct. Biol. 2008; 18:658–666. [PubMed: 19059104]
4. Drennan CL, Huang S, Drummond JT, Matthews RG, Ludwig ML. How a Protein Binds B12: A 3.0 Å X-ray Structure of B12-Binding Domains of Methionine Sythase. Science. 1994; 266:1669–1674. [PubMed: 7992050]
5. Dixon MM, Huang S, Matthews RG, Ludwig ML. The Structure of the C-terminal Domain of Methionine Synthase: Presenting *S*-adenosylmethionine for Reductive Methylation of B12. Structure. 1996; 4:1263–1275. [PubMed: 8939751]
6. Doukov T, Seravalli J, Stezowski JJ, Ragsdale SW. Crystal Structure of a Methyltetrahydrofolate- and Corrinoid-Dependent Methyltransferase. Structure. 2000; 8:817–830. [PubMed: 10997901]
7. Bandarian V, et al. Domain Alternation Switches B12-Dependent Methionine Synthase to the Active Conformation. Nat. Struct. Biol. 2002; 9:53–56. [PubMed: 11731805]
8. Evans JC, et al. Structures of the N-terminal Module Imply Large Domain Motions During Catalysis by Methionine Synthase. Proc. Natl. Acad. Sci. U.S.A. 2004; 101:3729–3736. [PubMed: 14752199]
9. Svetlitchnaia T, Svetlitchnyi V, Meyer O, Dobbek H. Structural Insights into Methyltransfer Reactions of a Corrinoid Iron-Sulfur Protein Involved in Acetyl-CoA Synthesis. Proc. Natl. Acad. Sci. U.S.A. 2006; 103:14331–14336. [PubMed: 16983091]
10. Doukov TI, Hemmi H, Drennan CL, Ragsdale SW. Structural and Kinetic Evidence for an Extended Hydrogen-bonding Network in Catalysis of Methyl Group Transfer: Role of an Active Site Asparagine Residue in Activation of Methyl Transfer by Methyltransferases. J. Biol. Chem. 2007; 282:6609–6618. [PubMed: 17172470]
11. Datta S, Koutmos M, Pattridge KA, Ludwig ML, Matthews RG. A Disulfide-Stabilized Conformer of Methionine Synthase Reveals an Unexpected Role for the Histidine Ligand of the Cobalamin Cofactor. Proc. Natl. Acad. Sci. U.S.A. 2008; 105:4115–4120. [PubMed: 18332423]
12. Koutmos M, Datta S, Pattridge KA, Smith JL, Matthews RG. Insights into the Reactivation of Cobalamin-Dependent Methionine Synthase. Proc. Natl. Acad. Sci. U.S.A. 2009; 106:18527–18532. [PubMed: 19846791]
13. Banerjee RB, Matthews RG. Cobalamin-Dependent Methionine Synthase. FASEB J. 1990; 4:1450–1459. [PubMed: 2407589]
14. Ragsdale SW, Pierce E. Acetogenesis and the Wood-Ljungdahl Pathway of CO2 Fixation. Biochim. Biophys. Acta. 2008; 1784:1873–1898. [PubMed: 18801467]
15. Schrauzer GN, Deutsch E. Reactions of Cobalt(I) Supernucleophiles: The Alkylations of Vitamin B12s, Cobaloximes(I), and Related Compounds. J. Am. Chem. Soc. 1969; 91:3341–3350. [PubMed: 5791925]

16. Harder SR, Lu W-P, Feinberg BA, Ragsdale SW. Spectroelectrochemical Studies of the Corrinoid/Iron-Sulfur Protein Involved in Acetyl Coenzyme A Synthesis by *Clostridium thermoaceticum*. Biochemistry. 1989; 28:9080–9087. [PubMed: 2605242]
17. Banerjee RB, Harder SR, Ragsdale SW, Matthews RG. Mechanism of Reductive Activation of Cobalamin-Dependent Methionine Synthase: An Electron Paramagnetic Resonance Spectroelectrochemical Study. Biochemistry. 1990; 29:1129–1135. [PubMed: 2157485]
18. Menon S, Ragsdale SW. Role of the [4Fe-4S] Cluster in Reductive Activation of the Cobalt Center of the Corrinoid Iron-Sulfur Protein from *Clostridium thermoaceticum* during Acetate Biosynthesis. Biochemistry. 1998; 37:5689–5698. [PubMed: 9548955]
19. Menon S, Ragsdale SW. The Role of an Iron-Sulfur Cluster in an Enzymatic Methylation Reaction. J. Biol. Chem. 1999; 274:11513–11518. [PubMed: 10206956]
20. Zydowsky TM, et al. Stereochemical Analysis of the Methyl Transfer Catalyzed by Cobalamin-Dependent Methionine Synthase from *Escherichia coli* B. J. Am. Chem. Soc. 1986; 108:3152–3153.
21. Ragsdale SW, Lindahl PA, Münck E. Mössbauer, EPR, and Optical Studies of the Corrinoid/Iron-Sulfur Protein Involved in the Synthesis of Acetyl Coenzyme A by *Clostridium thermoaceticum*. J. Biol. Chem. 1987; 262:14289–14297. [PubMed: 2821001]
22. Zhao S, Roberts DL, Ragsdale SW. Mechanistic Studies of the Methyltransferase from *Clostridium thermoaceticum*: Origin of the pH Dependence of the Methyl Group Transfer from Methyltetrahydrofolate to the Corrinoid/Iron-Sulfur Protein. Biochemistry. 1995; 34:15075–15083. [PubMed: 7578120]
23. Seravalli J, Zhao S, Ragsdale SW. Mechanism of Transfer of the Methyl Group from (*6S*)-Methytetrahydrofolate to the Corrinoid/Iron-Sulfur Protein Catalyzed by the Methyltransferase from *Clostridium thermoaceticum*: A Key Step in the Wood-Ljungdahl Pathway of Acetyl-CoA Synthesis. Biochemistry. 1999; 38:5728–5735. [PubMed: 10231523]
24. Jarrett JT, et al. Mutations in the B12-Binding Region of Methionine Synthase: How the Protein Controls Methylcobalamin Reactivity. Biochemistry. 1996; 35:2464–2475. [PubMed: 8652590]
25. Bandarian V, Ludwig ML, Matthews RG. Factors Modulating Conformational Equilibria in Large Modular Proteins: A Case Study with Cobalamin-Dependent Methionine Synthase. Proc. Natl. Acad. Sci. U.S.A. 2003; 100:8156–8163. [PubMed: 12832615]
26. Wirt MD, et al. Structural and Electronic Factors in Heterolytic Cleavage: Formation of the Co(I) Intermediate in the Corrinoid/Iron-Sulfur Protein from *Clostridium thermoaceticum*. Biochemistry. 1995; 34:5269–5273. [PubMed: 7711048]
27. Stich TA, et al. Spectroscopic Studies of the Corrinoid/Iron-Sulfur Protein from *Moorella thermoacetica*. J. Am. Chem. Soc. 2006; 128:5010–5020. [PubMed: 16608335]
28. Elliott JI, Brewer JM. The Inactivation of Yeast Enolase by 2,3-butanedione. Arch. Biochem. Biophys. 1978; 190:351–357. [PubMed: 360996]
29. Otwinowski Z, Minor W. Processing of X-ray Diffraction Data Collected in Oscillation Mode. Methods Enzymol. 1997; 276:307–326.
30. McCoy AJ, et al. *Phaser* Crystallographic Software. J. Appl. Cryst. 2007; 40:658–674. [PubMed: 19461840]
31. Brünger AT, et al. *Crystallography & NMR System*: A New Software Suite for Marcromolecular Structure Determination. Acta Cryst. 1998; D54:905–921.
32. Adams PD, et al. *PHENIX*: A Comprehensive Python-Based System for Macromolecular Structure Solution. Acta Cryst. 2010; D66
33. Emsley P, Lohkamp B, Scott WG, Cowtan K. Features and Development of Coot. Acta Cryst. 2010; D66:486–501.
34. Laskowski RA, MacArthur MW, Thornton JM. PROCHECK: A Program to Check the Stereochemical Quality of Protein Structures. J. Appl. Cryst. 1993; 26:283–291.
35. Lu W-P, Schiau I, Cunningham JR, Ragsdale SW. Sequence and Expression of the Gene Encoding the Corrinoid/Iron-Sulfur Protein from *Clostridium thermoaceticum* and Reconsitution of the Recombinant Protein to Full Activity. J. Biol. Chem. 1993; 268:5605–5614. [PubMed: 8449924]

36. Ljungdahl LG, LeGall J, Lee J-P. Isolation of a Protein Containing Tightly Bound 5-Methoxybenzimidazolylcobamide (Factor IIIm) from *Clostridium thermoaceticum*. Biochemistry. 1973; 12:1802–1808. [PubMed: 4699238]

37. Zehnder AJB, Wuhrmann K. Titanium(III) Citrate as a Nontoxic Oxidation-Reduction Buffering System for the Culture of Obligate Anaerobes. Science. 1976; 194:1165–1166. [PubMed: 793008]

38. Royant A, et al. Advances in Spectroscopic Methods for Biological Crystals. 1. Fluorescence Lifetime Measurements. J. Appl. Cryst. 2007; 40:1105–1112.

39. Barstow B, Ando N, Kim CU, Gruner SM. Alteration of Citrine Structure by Hydrostatic Pressure Explains the Accompanying Spectral Shift. Proc. Natl. Acad. Sci. U.S.A. 2008; 105:13362–13366. [PubMed: 18768811]

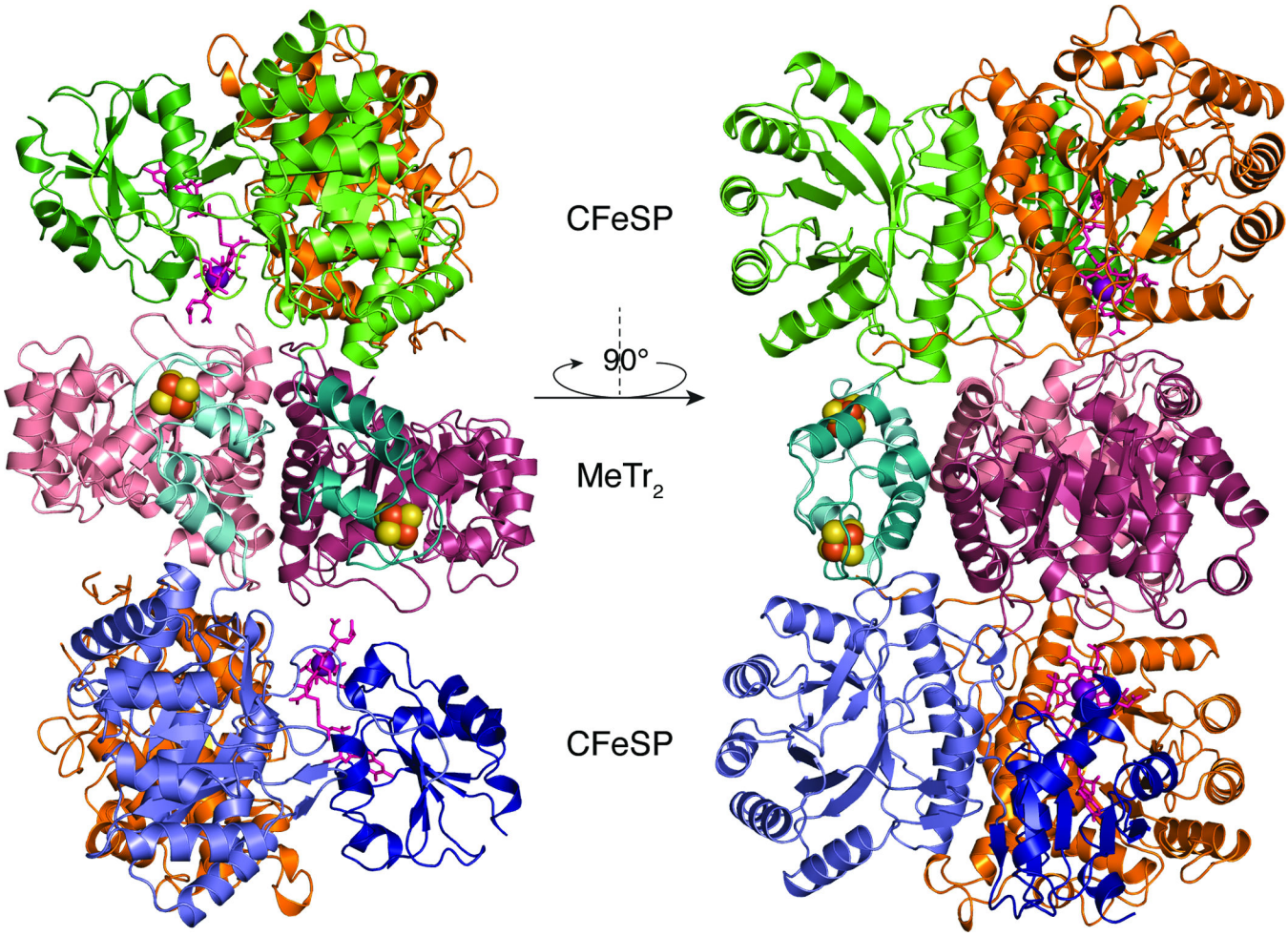

Figure 1. The overall CFeSP/MeTr complex

Ribbon representation of MeTr homodimer ($MeTr_2$) in light and dark pink, CFeSP small subunits in orange, and CFeSP large subunit Fe_4S_4 domains in teal and cyan, TIM barrel domains in green and blue, and B_{12}-domains in dark green and dark blue. B_{12} cofactors in magenta sticks with cobalt as violet spheres. Fe_4S_4 clusters in spheres: Fe in orange and S in yellow.

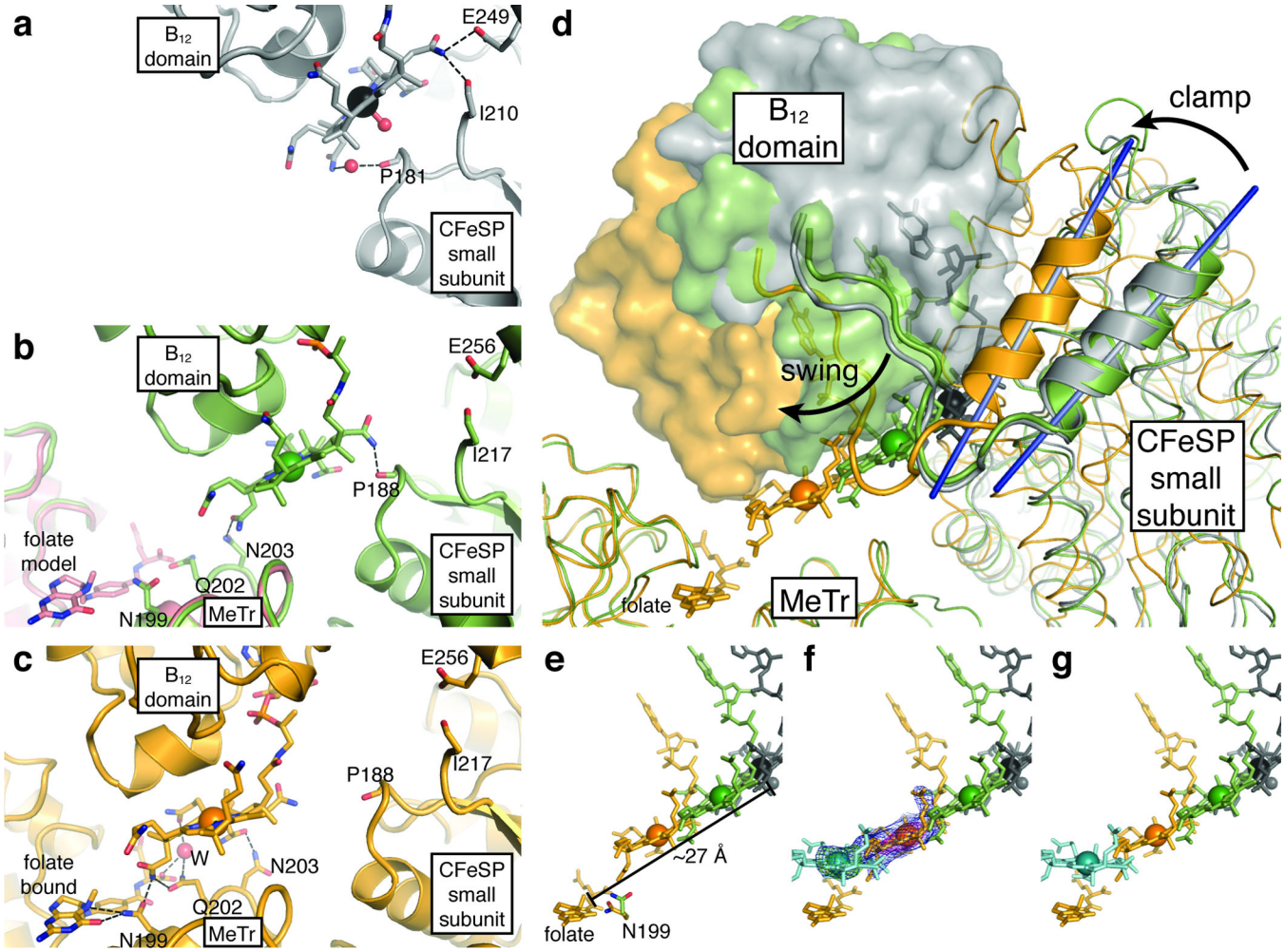

Figure 2. Comparison of B_{12} positions in "resting" *Ch*CFeSP, folate-free, and folate-bound CFeSP/MeTr

a, *Ch*CFeSP (grey ribbons, Co of B_{12}: black sphere). **b**, Folate-free CFeSP/MeTr (green ribbons, Co of B_{12}: green sphere) superimposed with CH_3-H_4folate-bound MeTr (PDB ID: 2E7F, pink ribbons). **c**, Folate-bound CFeSP/MeTr (orange ribbons, Co of B_{12}: orange sphere). Panels **a**–**c** are identical in orientation, B_{12} sticks coloured C: ribbon colour, O: red, N: blue, and P: orange. **d**, Superposition of *Ch*CFeSP (grey), folate-free CFeSP/MeTr (green), and folate-bound CFeSP/MeTr (orange) structures in **a**–**c**, highlighting one helix (thick ribbons) to show clamping motion (helix axes as straight blue lines) and B_{12} (sticks) with 12 residue linker (thick ribbons) to B_{12} domain (surface) to show swinging motion. **e**, Superposition of B_{12} and CH_3-H_4folate in **d**, with Asn199 shown for CFeSP/MeTr structures in sticks (C: ribbon colour, O: red, N: blue). **f**, Same as **e**, with $2F_o$-F_c density in blue (1.0 σ) and pink mesh (4.0 σ), and F_o-F_c density in green mesh (3.0 σ) for folate-bound CFeSP/MeTr structure. Putative alternative B_{12} corrin: cyan. **g**, Superposition of B_{12} cofactors and CH_3-H_4folate in **f**.

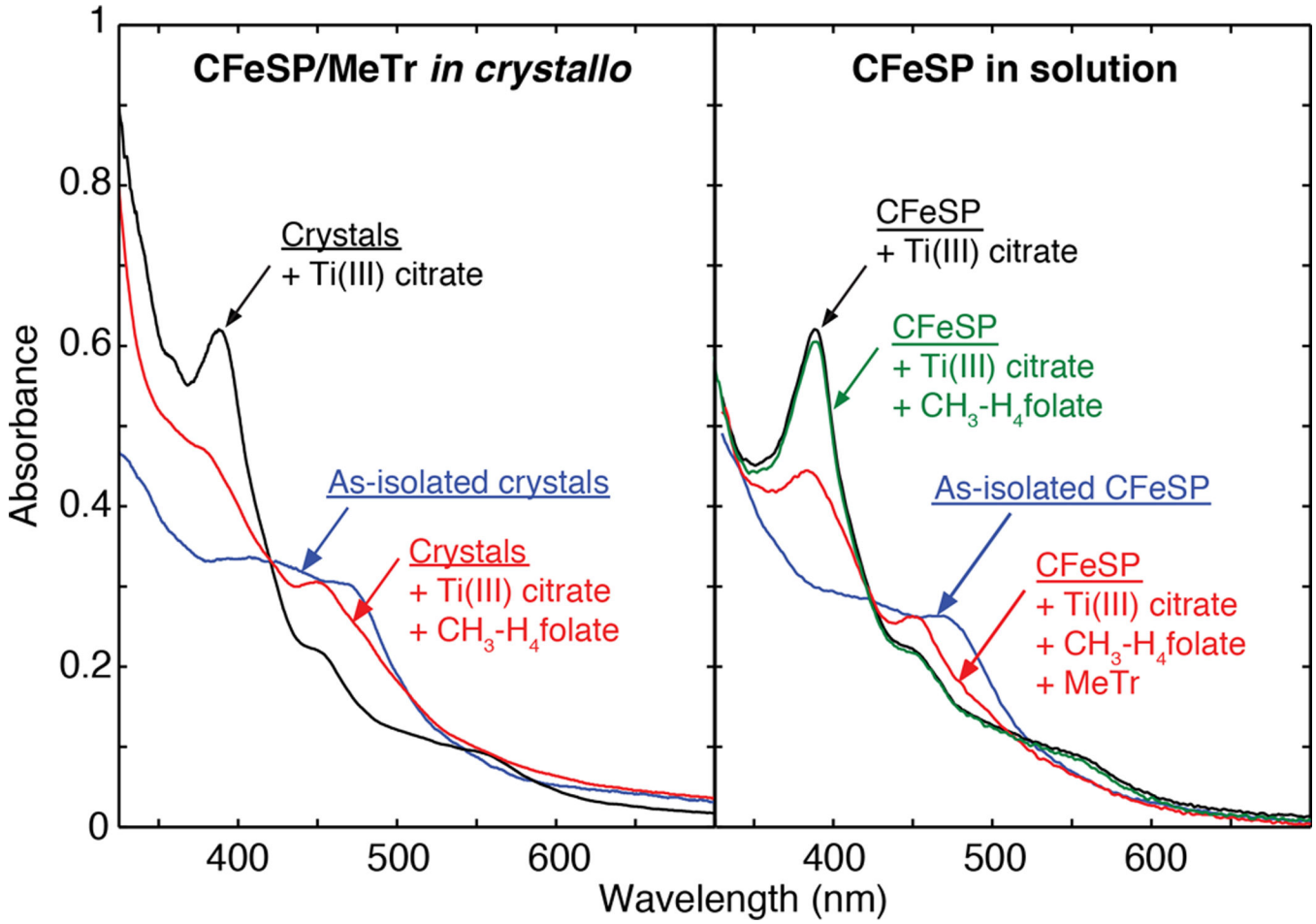

Figure 3. Methyltransfer activity of CFeSP/MeTr crystals by UV-vis absorption spectroscopy

As-isolated spectra (blue lines) for CFeSP/MeTr crystals and CFeSP in solution similarly have broad features at ~400 nm and ~470 nm arising from the Fe_4S_4 cluster and the B_{12} corrin. Following established protocols[18,19,22,23,26,27], B_{12} reduction was achieved with Ti(III) citrate, yielding a sharp 390 nm peak indicative of active Co(I) in both solution and *in crystallo* spectra (black lines). Further treatment with CH_3-H_4folate yields decreased absorbance at 390 nm and a new peak at 450 nm (red lines), characteristic of the product complex (protein-bound CH_3-Co(III)[18,19,22,23]). A control reaction (green line) confirms that turnover does not occur from free CH_3-H_4folate without MeTr, and the 450 nm peak indicates that B_{12} remains CFeSP-bound (free B_{12} has a peak at ~520 nm instead[18,21,27]).

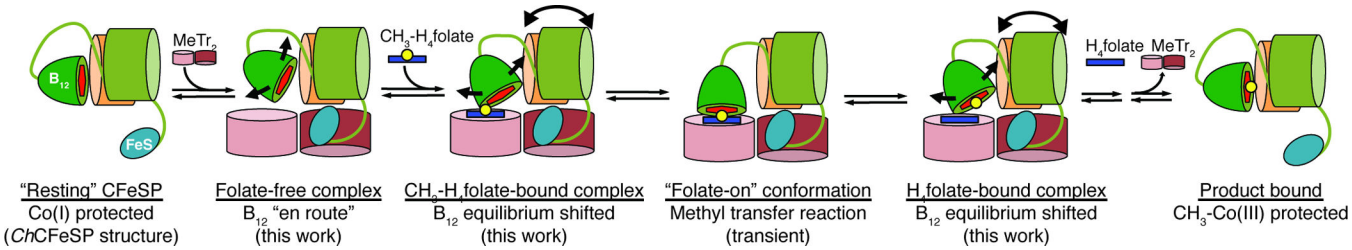

Figure 4. Cartoon model of B_{12}-dependent methyltransfer in CFeSP/MeTr

For simplicity, only one of the two CFeSP heterodimers is shown. Protein domains are colored as in Fig. 1, loops represent linkers, red hexagon is B_{12}, blue rectangle is folate, and transferred methyl group is shown as a yellow sphere. Curved arrows denote "swinging" and "clamping" motions.